Journal of Physiology (1990), **421**, *pp.* 499–519
With 11 *figures*
Printed in Great Britain

INOSITOL TRISPHOSPHATE MEDIATES CLONED MUSCARINIC RECEPTOR-ACTIVATED CONDUCTANCES IN TRANSFECTED MOUSE FIBROBLAST A9 L CELLS

BY S. V. PENELOPE JONES, JEFFERY L. BARKER, MIRIAM B. GOODMAN AND MARK R. BRANN

From the Laboratory of Neurophysiology and the Laboratory of Molecular Biology, National Institute of Neurological Disorders and Stroke, National Institutes of Health, Bethesda, MD 20892, USA

(*Received 22 March 1989*)

SUMMARY

1. The mechanism by which cloned m1 and m3 muscarinic receptor subtypes activate Ca^{2+}-dependent channels was investigated with whole-cell and cell-attached patch-clamp recording techniques and with Fura-2 Ca^{2+} indicator dye measurements in cultured A9 L cells transfected with rat m1 and m3 cDNAs.

2. The Ca^{2+}-dependent K^+ and Cl^- currents induced by muscarinic receptor stimulation were dependent on GTP. Responses were reduced when GTP was excluded from the intracellular recording solution or when GDP-β-S was added. Intracellular GTP-γ-S activated spontaneous fluctuations and permitted only one acetylcholine-(ACh) induced current response. These results implicate GTP-binding proteins (G protein) in the signal transduction pathway. This G protein is probably not pertussis toxin-sensitive as the ACh-induced electrical response was not abolished by pertussis toxin treatment.

3. Cell-attached single-channel recordings revealed activation of ion channels within the patch during application of ACh outside the patch, implying that second messengers might be involved in the ACh-induced response. Two types of K^+ channel were activated, a discrete channel of 36 pS and channel activity calculated to be about 5 pS.

4. Application of 8-bromo cyclic AMP or 1-oleoyl-1,2-acetylglycerol (OAG) produced no electrical response and did not affect the ACh-induced responses. Phorbol myristic acetate (PMA) evoked no electrical response, but reduced the ACh-induced responses.

5. Inclusion of inositol 1,4,5-trisphosphate (IP_3) in the intracellular pipette solution activated outward currents at -50 mV associated with an increase in conductance. The IP_3-induced current response reversed polarity at -65 mV and showed a dependence on K^+. Increasing the intracellular free Ca^{2+} concentration ($[Ca^{2+}]_i$) from 20 nM to 1 μM also induced an outward current response associated with an increase in conductance. Inclusion of inositol 1,3,4,5-tetrakisphosphate (IP_4) in the intracellular solution had no effect on the A9 L cells.

6. Fura-2 measurements revealed ACh-induced increases in Ca_i^{2+}. The Ca^{2+} responses were abolished by atropine showing that they were muscarinic in nature.

Removal of extracellular Ca^{2+} did not affect the initial ACh-induced increase in Ca_i^{2+} but subsequent Ca_i^{2+} responses to ACh were depressed, suggesting depletion of Ca^{2+} intracellular stores. Residual though small responses continued to be elicited by ACh. Barium (5 mM) had little effect and cobalt slightly reduced the ACh-induced Ca^{2+} response.

7. The ACh-induced currents recorded at −50 mV were unaffected by removal of extracellular Ca^{2+}.

8. It is concluded that a pertussis toxin-insensitive G protein is involved in the m1 and m3 ACh-induced electrical response. Inclusion of IP_3 in the intracellular solution or elevated Ca_i^{2+} mimicked the ACh-induced current response. The ACh-induced electrical responses were not dependent on extracellular Ca^{2+}, suggesting that IP_3 releases Ca^{2+} from intracellular stores, which in turn activates the Ca^{2+}-dependent conductances. Cyclic AMP and diacylglycerol (DAG) produce no electrical response and do not affect the ACh-induced currents.

INTRODUCTION

Muscarinic receptors are widely distributed throughout the nervous system, where they are coupled to a variety of physiological responses (for reviews see Brown, 1986; Harden, Tanner, Martin, Nakahata, Hughes, Hepler, Evans, Masters & Brown, 1986; Nathanson, 1987; Christie & North, 1988; Nicoll, 1988). Five subtypes of muscarinic receptor have been cloned (m1–m5) (Kubo, Fukuda, Mikami, Maeda, Takahashi, Mishina, Haga, Haga, Ichiyama, Kangawa, Kojima, Matsuo, Hirose & Numa, 1986; Bonner, Buckley, Young & Brann, 1987; Kubo, Maeda, Sugimoto, Akiba, Mikami, Takahashi, Haga, Haga, Ichiyama, Kangawa, Matsuo, Hirose & Numa, 1987; Peralta, Ashkenazi, Winslow, Smith, Ramachandran & Capon, 1987; Bonner, Young, Brann & Buckley, 1988).

The signals transduced by each of these cloned muscarinic receptor subtypes have been studied recently. Receptors m1 and m3 activate Ca^{2+}-dependent K^+ and Cl^- conductances when expressed in A9 L cells (Jones, Barker, Bonner, Buckley & Brann, 1988*a*; Jones, Barker, Buckley, Bonner, Collins & Brann, 1988*b*) and inhibit the M-current as well as activating Ca^{2+}-dependent K^+ conductances, when expressed in NG108-15 cells (Fukuda, Higashida, Kubo, Maeda, Akiba, Bujo, Mishina & Numa, 1988). The m2 receptor has been associated with activation of a cation conductance and a Ca^{2+}-dependent Cl^- conductance in *Xenopus* oocytes (Fukuda, Kubo, Akiba, Maeda, Mishina & Numa, 1987), whilst no electrical function has been recorded when m2 or m4 have been expressed in A9 L or NG108-15 cells (Fukuda *et al.* 1988; Jones *et al.* 1988*b*). Stimulation of m1, m3 and m5 results in activation of phospholipase C, increases in cyclic AMP (Brann, Conklin, Dean, Collins, Bonner & Buckley, 1988; Jones, Murphy & Brann, 1989*b*) and enhanced arachidonic acid release (Conklin, Brann, Buckley, Ma, Bonner & Axelrod, 1988). In A9 L cells, m2 and m4 do not affect phospholipase C or arachidonic acid release, but decrease cyclic AMP levels (Jones *et al.*, 1989*b*; Novotny & Brann, 1989). In human kidney cells, however, m2 and m4 receptors activate phospholipase C but with much lower

efficiency than do m1 and m3 receptors (Peralta, Ashkenazi, Winslow, Ramachandran & Capon, 1988).

The current study examines the mechanism by which muscarinic receptors activate Ca^{2+}-dependent K^+ and Cl^- conductances in A9 L cells transfected with m1 and m3 muscarinic receptor subtypes. Some of the results presented here have been published in abstract form (Jones, Goodman, Barker & Brann, 1989*a*).

METHODS

Transfection and culture

The A9 L cell lines containing m1 and m3 muscarinic receptors used in this study are the same lines as studied previously (Jones *et al.* 1988*a*, *b*). The method of transfection of the A9 L cells involved co-transfection of muscarinic receptor cDNAs derived from rat brain (Bonner *et al.* 1987) with a plasmid containing the neomycin resistance gene as previously described (Brann, Buckley, Jones & Bonner, 1987). The levels of m1 and m3 receptors were 509 and 401 fmol mg^{-1} protein respectively, as measured by [^{3}H]QNB (quinuclidinyl benzylate) binding.

Electrophysiology and solutions

The A9 L cells were incubated at 37 °C in 95% air and 5% CO_2 in Dulbecco's modified Eagle's medium with 10% fetal calf serum for at least 24 h prior to recording. The cells were studied at room temperature (21–23 °C) on the inverted stage of a phase-contrast microscope at a magnification of ×320. The cell-attached and whole-cell recording techniques were used to record membrane currents and potentials, using a LIST EPC-7 amplifier (Hamill, Marty, Neher, Sakmann & Sigworth, 1981). The patch electrodes were made from thin-wall capilliary borosilicate glass (World Precision Instruments, CT, USA) and pulled on a two-stage horizontal electrode puller (Mecanex, Basel, Switzerland). Electrodes for use in cell-attached single-channel recordings were coated with Sylgard and fire-polished. Pipette resistances were 4–10 MΩ when placed in the bath and varied with pipette solution. Pipette seals of 5–20 GΩ were obtained before disruption of the membrane patch. Once access to the cell interior was established, cell input resistances of 1–3 GΩ were obtained at resting potential (~ -50 mV). Series resistance compensation was applied in voltage clamp.

The ionic composition of the extracellular medium was (in mM): 140 NaCl, 5 KCl, 5 HEPES, 5·6 D-glucose, 2 $CaCl_2$, 1 $MgCl_2$, pH adjusted to 7·4 with NaOH. The osmolarity was adjusted to 330–335 mosM with sucrose. Other extracellular solutions used include a high K^+ medium containing (in mM): 150 KCl, 5 HEPES, 2 $CaCl_2$, 1 $MgCl_2$, 5·6 D-glucose. In most experiments the intracellular patch pipette solution contained (in mM): 150 potassium gluconate, 2 $MgCl_2$, 5 HEPES, 1·1 EGTA, 0·1 $CaCl_2$, 5 Mg-ATP, 0·1 Li-GTP, pH adjusted to 7·2 with KOH. The osmolarity was adjusted to 320–325 mosM with sucrose. The free Ca^{2+} concentration was estimated to be about 20 nM (Fabiato & Fabiato, 1979).

Liquid-junction potentials between the bath solution and intracellular electrode solutions were eliminated by filling a side bath containing the reference electrode with the intracellular solution. Connections between the two baths were made via a low-resistance agar bridge.

Membrane currents were usually recorded from cells voltage clamped at −50 mV. Either resting current measurements were taken or the currents produced by a series of 10 mV, 100 ms, hyperpolarizing and depolarizing voltage steps applied at a frequency of 1 Hz were recorded. Acetylcholine (1–50 μM) or other substances were applied by low (1–2 lbf in^{-2}) pressure from a micropipette placed 5–10 μm from the cell. Acetylcholine pulses were usually applied at 3–4 min intervals, as this was sufficient time for recovery necessary to evoke constant amplitude current responses. The current and voltage responses were displayed on a Gould pen recorder (filtered at 50 Hz) and also sampled and digitized on-line by a PDP 11/23 mini-computer with an analog-to-digital Data Translation converter (12 bit, ±5 V range), at a digitization rate of 2·5 kHz. Signals were filtered at 1 kHz unless otherwise stated. Single-channel data were recorded on a Gould 6500 FM tape-recorder and subsequently amplified, filtered at 1 kHz (Frequency Devices, 902 8-pole Bessel filter) and digitized at 2 kHz using an IBM PC AT computer with an analog-to-digital

Cambridge Electronic Design 1401 Laboratory interface. Single-channel analysis was performed by compilation of the distribution of current amplitude utilizing histograms of percentage of time spent at each of 512 current levels and fitting the zero and peak current levels using the single-channel analysis program PAT (Dempster, 1988) to obtain the unitary channel current. To determine single-channel conductance of data that displayed activation of multiple channels in the patch, the variance of the channel noise was calculated using the program SPAN (Dempster, 1988). As the ACh-induced current responses desensitized quite rapidly, a sufficient length of current could not be recorded from which to obtain Lorentzian spectra. Also, as the responses appeared to be all-or-none the criteria for a low probability of channel opening is not necessarily obeyed. Instead the DC current was measured by averaging every 512 points and the variance calculated for each portion of equivalent AC current. Using the relationship between the variance of the signal and mean current, single-channel conductance (γ) can be calculated by

$$\gamma = \sigma^2/(I_m(V - V_r)),$$

where σ^2 is the signal variance, I_m is the mean DC current, V is holding potential and V_r is the equilibrium potential of the ion involved. For noise analysis single-channel currents were low-pass filtered at 1 kHz (Frequency Devices, 8-pole Butterworth) and high pass at 4 Hz (Frequency Devices, 2-pole Butterworth), amplified and digitized at 2 kHz (CED 1401). Data with correlation coefficients of variance to mean current of less than 0·8 were rejected.

Antagonists were applied directly to the bath and solution changes were obtained by perfusion of the 1·5 ml bath (Forsythe & Coates, 1988) with fresh medium at a flow rate of 2 ml min^{-1}. All results are expressed as mean ± standard error of the mean.

Optical recordings of Fura-2 fluorescence

Loading the A9 L cells with the Ca^{2+}-sensitive dye, Fura-2, was accomplished by incubation with Fura-2 acetoxymethyl ester (Fura-2 AM, 0·5–1 μM) for 30 min in the above extracellular recording solution supplemented with 1 mM-probenecid. Probenicid is an antagonist of acid transport systems and aids dye loading (Di Virgilio, Steinberg, Swanson & Silverstein, 1988). After loading, the cultures were washed and allowed to de-esterify for 30–60 min. Single-cell quantitative fluorescence microscopy was performed with a microcomputer-controlled microscope (Zonax, Carl Zeiss, Thornwood, NY, USA) and a Zeiss Plan-Neofluar 25 × /0·8 numerical aperture objective. The microscope was equipped with a 100 W mercury arc lamp, epi-fluorescence and phase contrast optics. Bandpass filters at 340 and 380 nM (Oriel) were alternately placed in the light path by a custom-built filter flipper to provide excitation for Fura-2 fluorescence. A ratio was measured every 918 ms. Fluorescence emission intensity was measured at 500–510 nm with a photomultiplier tube and restricted to the cell of interest by an emission aperture. In addition, a pinhole in the illumination path restricted UV illumination to about 15% of the visual field, minimizing light-induced cell damage. Drugs were applied by rapid perfusion of the bath (~ 3 ml min^{-1}). Following the general procedure outlined in Grynkiewcz, Poenie & Tsien (1985), Fura-2 calibrations were occasionally obtained in this cell type. Calibration of Fura-2 fluorescence in terms of Ca^{2+} concentration was performed by exposing the cells to 10 μM-ionomycin initially in Ca^{2+}-free medium (containing (mM): 140 NaCl, 5 KCl, 1 $MgCl_2$, 5 glucose, 5 HEPES, 1·1 EGTA, pH adjusted to 7·4) followed by a Ca^{2+}-containing medium (in mM: 140 NaCl, 5 KCl, 2 $CaCl_2$, 1 $MgCl_2$, 5 glucose, 5 HEPES). This protocol produced reproducible results, but required approximately 1 h to yield stable values. Over such an extended period, photo-bleaching significantly reduced the fluorescence signal at both 340 and 380 nm excitation, introducing errors into the process of calibration. Therefore, calibration was not performed routinely. Only those experiments where calibration values could be determined in a timely fashion in the same cell are expressed in terms of $[Ca^{2+}]_i$. The remainder of the data are expressed as the ratio of fluorescence measured at 340 nm (Ca^{2+}-bound Fura-2) divided by the fluorescence at 380 nm (free Fura-2).

Drugs

Acetycholine chloride, atropine sulphate, Mg-ATP, phorbol 12-myristate 13-acetate, 8-bromo cyclic AMP and probenicid were obtained from Sigma Chemical Company (St Louis, MO, USA). Li-GTP, Li-GDP-β-S and Li-GTP-γ-S were obtained from Boehringer Mannheim (FRG). Inositol 1,4,5-trisphosphate (IP_3) and inositol 1,3,4,5-tetrakisphosphate (IP_4) were obtained from Calbiochem

Corp. (La Jolla, CA, USA). 1-Oleoyl-1,2-acetylglycerol (OAG) and Fura-2 were obtained from Molecular Probes (Eugene, OR, USA).

RESULTS

Involvement of G proteins in responses to ACh

Application of 1–50 μM-ACh from a pressure ejection pipette elicited slightly delayed (2–3 s) outward current responses in A9 L cells transfected with either m1

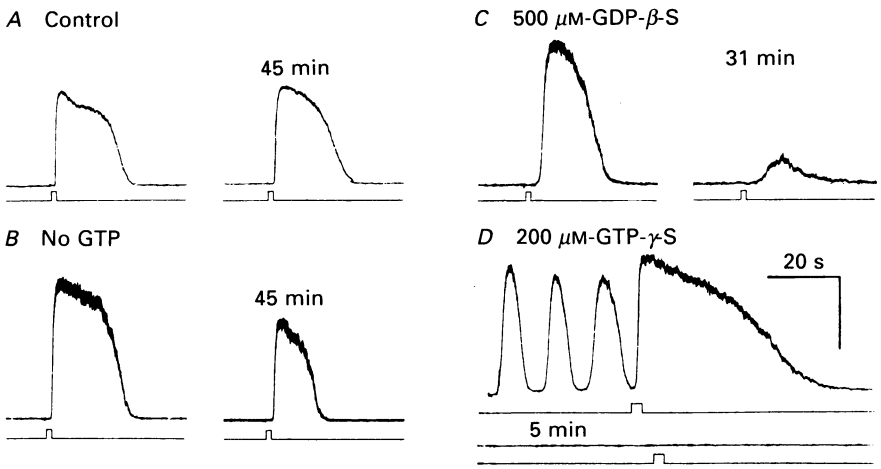

Fig. 1. ACh-induced response is mediated via G protein activation. Outward currents were recorded in A9 L cells transfected with the m1 muscarinic receptor subtype, voltage clamped at −50 mV in *A* and *D*, and at −30 mV in *B* and *C*. Acetylcholine (10 μM) was applied at times indicated in lower traces. *A*, under control conditions with 5 mM-ATP and 0·1 mM-GTP in the intracellular pipette solution, responses remained constant in amplitude and duration for at least 45 min. *B*, in the absence of GTP in the intracellular solution the ACh-induced current slowly waned. *C*, ACh-induced currents declined faster and to a greater extent when recorded with pipette solutions lacking GTP and to which 500 μM-GDP-β-S had been added. *D*, spontaneous repetitive current oscillations occurred when 200 μM-GTP-γ-S was included in the patch pipette. Initial ACh-induced responses were full in amplitude and often prolonged, but could not be re-evoked on second application of ACh (see lower pair of traces). Times shown in minutes with each panel indicate time elapsed since initial response. Vertical calibration: *A*, 100 pA; *B–D*, 50 pA.

or m3 muscarinic receptor cDNAs, when voltage clamped in whole-cell mode at −50 mV. Similar though slightly smaller delays in current development were seen by Horn & Marty (1988) in response to Ach in lacrimal glands, when recorded in nystatin-treated whole-cell recordings. The amplitude and duration of the outward currents induced by ACh in this study remained constant over a period of up to about 2 h, if 2–3 s pulses of ACh were applied about every 3 min (Figs 1*A* and 2). Application of ACh in pulses longer than this did not greatly prolong the response and in fact continual application of ACh did not alter the time course of the response which declined within about 25 s.

Concentrations of 20 nM to 50 μM-ACh produced maximal current responses, whilst lower concentrations tested did not elicit current responses (Jones *et al.* 1988*b*); thus responses appear to be all or none.

The intracellular pipette solutions for control experiments (Fig. 1*A*) contained potassium gluconate (see Methods) to which had been added 5 mM-ATP and 0·1 mM-GTP. When recorded with intracellular pipette solutions lacking in ATP, the amplitude of the ACh-induced current responses declined rapidly (around 10 min,

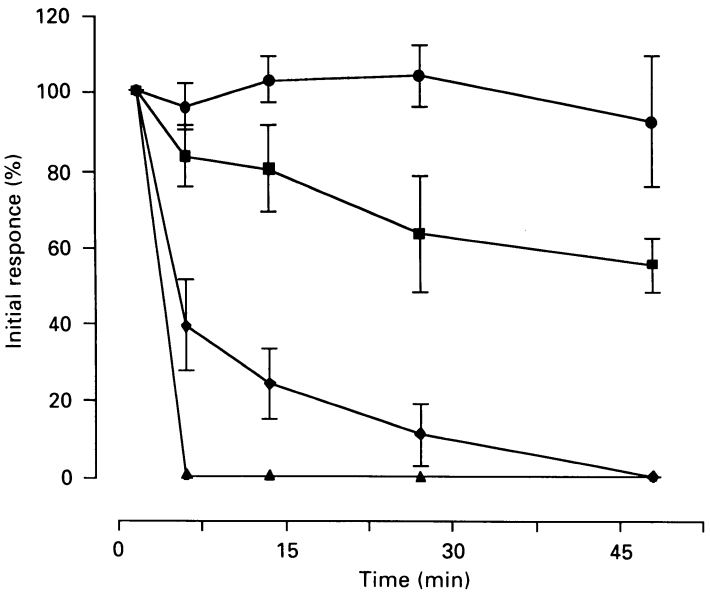

Fig. 2. Time course of the effects of various intracellularly applied GDP and GTP analogues on ACh-induced current amplitude. Control (●); No GTP (■); 500 μM-GDP-β-S (◆); 200 μM-GTP-γ-S (▲); expressed as percentage peak amplitude of first response. Data points represent mean ± S.E.M. of at least six experiments.

not shown). The ACh-induced responses also declined with time when recorded with intracellular pipette solutions lacking in GTP (Figs 1*B* and 2), dropping in amplitude to 77 ± 5% ($n = 5$) of the initial response within 20 min. In the absence of GTP, addition of a non-hydrolysable analogue of GDP, GDP-β-S (500 μM), to the intracellular medium produced a greater run-down of the ACh-induced outward current responses (Fig. 1*C*) in comparison to that obtained with recordings lacking in GTP (Fig. 2). The current amplitude dropped to 45 ± 9% ($n = 6$) of the initial response in 10 min in cells recorded with GDP-β-S. Inclusion of the non-hydrolysable analogue of GTP, GTP-γ-S, in the intracellular medium evoked an increase in the spontaneous activation of outward currents in nine out of fourteen cells upon rupture of the patch and entry into the whole-cell mode (Fig. 1*D*). Application of ACh under these conditions often elicited responses which were prolonged in comparison to ACh-induced responses in control cells. A second application of ACh to GTP-γ-S-dialysed cells did not elicit a response whether applied 3 or 30 min after whole-cell recording mode was established (Fig. 2). Finally, incubation of the cells with 100 ng ml^{-1} of pertussis toxin (overnight) did not inhibit the responses to ACh ($n = 15$). This treatment had previously been shown to be effective, as assayed by inhibition of m2- and m4-induced reductions in cyclic AMP (Novotny & Brann, 1989). The results show that activation of a pertussis toxin-insensitive G protein is involved in the ACh-induced conductance increase.

ACh-induced channels can be activated indirectly

The coupling of the G protein to the Ca^{2+}-dependent K^+ and Cl^- conductances was further investigated using the cell-attached patch configuration. The cells were bathed in a high K^+-containing medium (see Methods) and cell-attached recordings were made with pipette solutions containing the same high K^+ solution. Application of 10 μM) ACh to the cell outside the patch elicited discrete channel activity in the isolated patch (Fig. 3*A*), demonstrating that activation of these channels can be indirect, presumably via diffusible second messengers. The channels reversed polarity at 0 mV (Fig. 3*B*) which under these experimental conditions is similar to that estimated for the K^+ equilibrium potential (0 mV, assuming 150 mM-intracellular K^+). The amplitude distributions of the single-channel currents at depolarized and hyperpolarized potentials were constructed to obtain average current levels, which were plotted against pipette potential (Fig. 3*C*). The slope of the single-channel current–voltage relationship gave a single-channel conductance of $36 \pm 1{\cdot}4$ pS ($n = 3$) in this solution. This channel type was observed in approximately one-third ($n = 12$) of cell-attached patches recorded.

A second type of channel activity was elicited on application of ACh to the cell in another third ($n = 13$) of all patches examined (Fig. 3*D*). This channel activity also reversed at 0 mV and thus may also involve K^+ ions. This activity was considerably more complex than that described above and multiple channel openings made the data difficult to analyse as discrete single-channel openings. An analysis of the variance of the ACh-induced channel noise was used to obtain the single-channel conductance. The mean DC current was sampled and averaged every 512 record points and is shown plotted against time in Fig. 4*A*. The variance for each 512-point section was calculated for both background and agonist-induced currents. A plot of the calculated variance of the AC coupled signal *versus* the mean DC current is shown in Fig. 4*B*. The background variance has been subtracted. Single-channel conductance (γ) can be estimated from the slope of the variance to mean current plot (see Methods). The single-channel conductance was calculated to be $5{\cdot}5 \pm 1{\cdot}2$ pS ($n = 5$). In the estimation of the conductance of this channel activity, no account was taken of the larger 36 pS channel. This was deemed unnecessary as the mean current amplitude in three of the five recordings from which γ was calculated was less than that of the larger 36 pS channel and the calculated γ for these three was $6{\cdot}1 \pm 2{\cdot}0$ pS. In the other two patches, where it is possible that one 36 pS channel was present, assuming that these had no effect on the variance but only on the mean current amplitude, a recalculation of the data using these two adjusted values gave $\gamma = 7{\cdot}8 \pm 1{\cdot}5$ pS ($n = 5$).

A third species of channel activity was recorded at 0 mV and thus was unlikely to be a K^+ channel (Fig. 3*E*). It was infrequently observed ($n = 3$) and the reversal potential was not established. Twelve percent ($n = 5$) of the patches examined ($n = 33$) did not display ACh-induced channel activity.

Responses to ACh are mediated via IP_3

From the several seconds delay characteristic of the electrical response to ACh in the whole-cell recordings, and from the results of the cell-attached patch recordings, it appears that ACh activates ion channels indirectly via a diffusable second

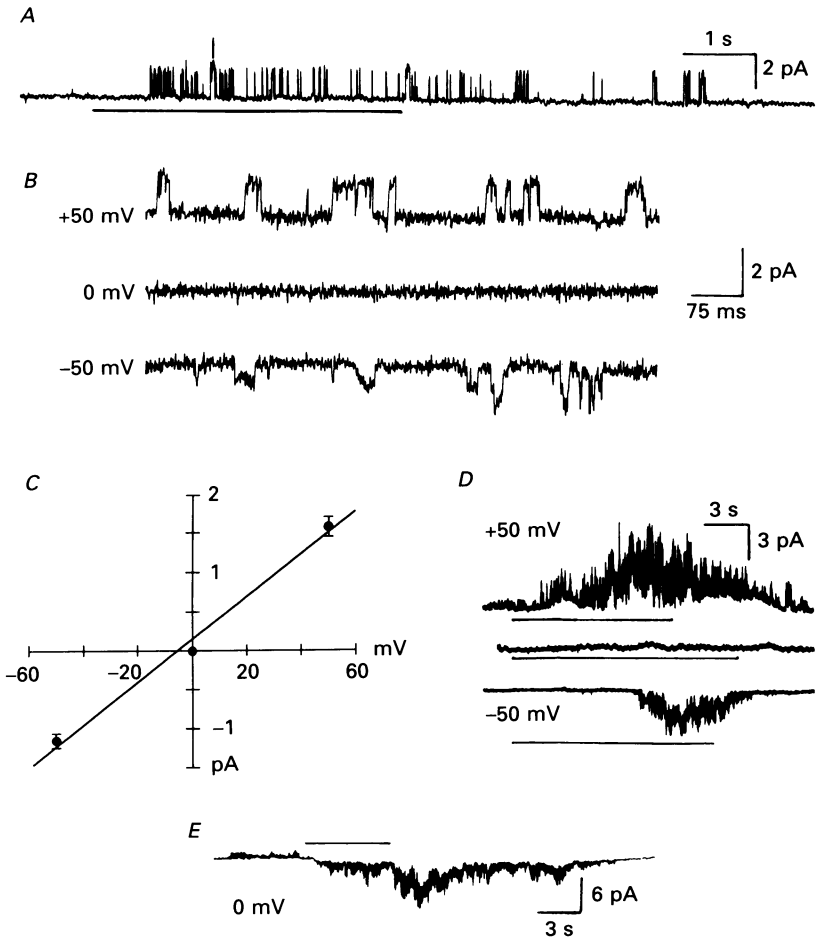

Fig. 3. Channel activity can be activated indirectly by ACh. Cell-attached patches were recorded with extracellular and patch electrode solutions containing 150 mM-KCl. *A*, application of 10 μM-ACh to the surface of the cell (marked by bar beneath) elicited channel activity lasting about 10 s after a delay of about 1 s. The patch was held at +50 mV. *B*, the ACh-induced channels reversed polarity at around 0 mV. *C*, a plot of single-channel current amplitude against patch potential gave a slope conductance of 36 pS. Data points show mean $\pm$ S.E.M. of three experiments. *D*, another type of ACh-induced channel activity was recorded which also reversed at 0 mV. From an analysis of the variance of the current noise the single-channel conductance was calculated to be about 5 pS. *E*, a third type of ACh-induced current was active at 0 mV, possibly a Cl^- conductance. Bars indicate pressure injection application of 10 μM-ACh to the cell surface. In no instance is the ACh present in the patch pipette solution. ACh-induced channel activity was similar in both m1 and m3-transfected cells.

messenger. Thus the effects of putative second messengers were investigated. 8-Bromo cyclic AMP (5 mM), a membrane-permeable analogue of cyclic AMP, produced no response when applied in the bathing medium from a pressure ejection pipette or when included in the patch pipette solution, and had no effect on the ACh-induced outward current ($n = 12$) (Fig. 5*A*). An analogue of DAG, OAG, elicited no response when applied from a pressure ejection pipette in concentrations ranging

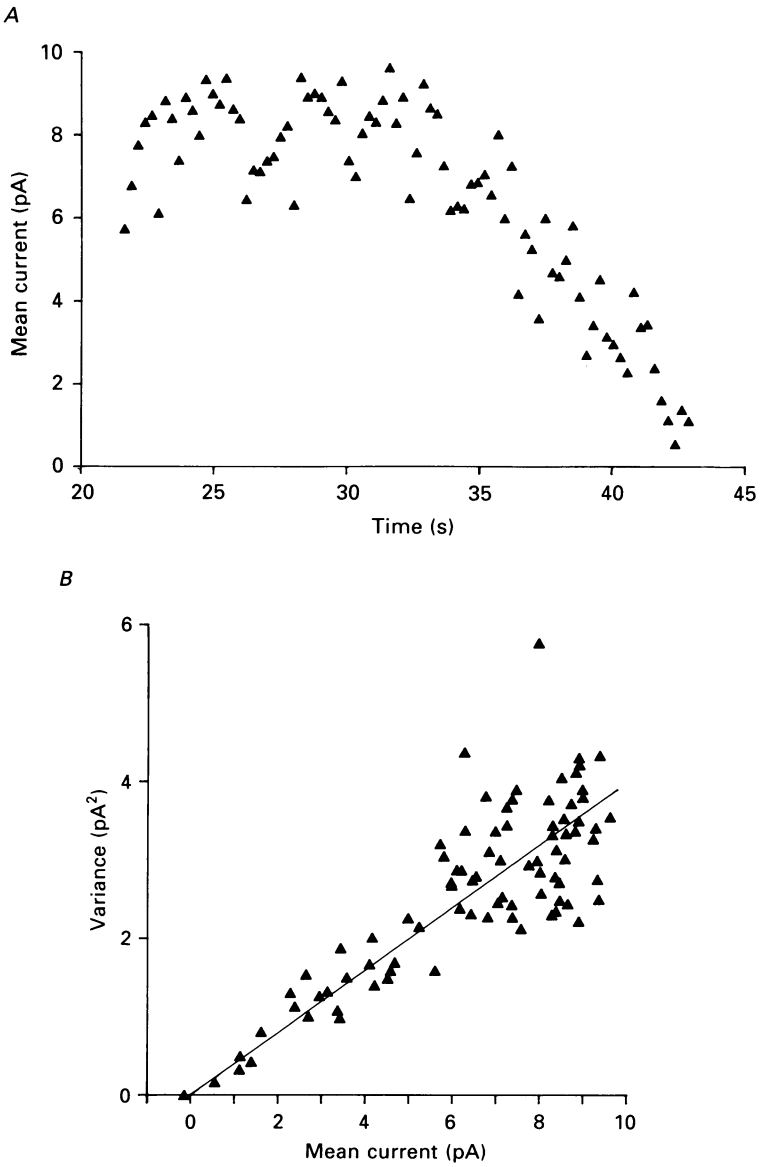

Fig. 4. Analysis of variance for single-channel noise measurements in the cell-attached patch mode. *A*, mean DC current is plotted as averages of 512 points against time of recorded agonist-induced signal. The baseline section corresponds to the first 20 s. *B*, variance calculated for each 512 point section of AC current is shown plotted against its corresponding DC current. The single-channel conductance was obtained from the slope divided by the driving force. The patch was held at 70 mV and in 150 mM-extracellular K^+, the reversal potential is about 0 mV. The correlation coefficient was 0·83.

from 5 to 50 μM ($n = 4$) and had no effect on the response to ACh (Fig. 5*B*). Inclusion of 5 μM-OAG in the intracellular pipette solution also had no effect on resting or agonist-induced properties ($n = 5$). PMA, which activates protein kinase C, did not alter the electrical properties of A9 L cells, but reproducibly and irreversibly reduced

the ACh-induced current amplitude to $61 \pm 10\%$ ($n = 11$) of the initial response within 10 min (Fig. 5*C*).

The possible roles of IP_3 and its metabolite IP_4 were investigated by including them in the intracellular pipette solution. After rupturing the patch to obtain the

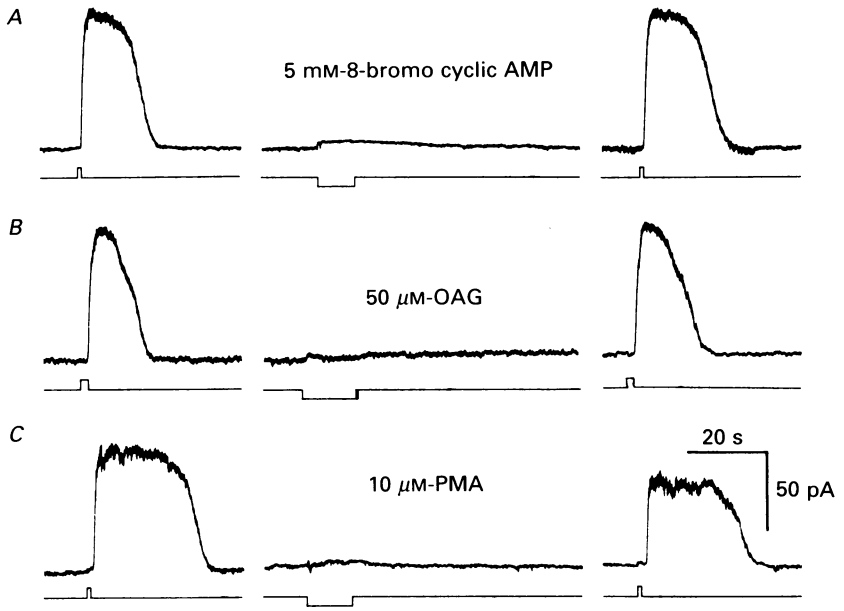

Fig. 5. ACh-induced currents are not mimicked by cyclic AMP, OAG or PMA. Current traces are shown from A9 L cells transfected with the m1 muscarinic receptor and voltage clamped at −50 mV. Application of 10 μM-ACh is shown as an upward deflection in the lower traces. *A*, application of 5 mM-8-bromo cyclic AMP (downward deflection in lower trace) produced no response and did not affect the ACh-induced responses. *B*, application of 50 μM-OAG also produced no response and had no effect on the ACh-induced responses. *C*, 10 μM-PMA had no electrical effect but caused an irreversible reduction in ACh-induced outward current amplitude in about 20–30 min. Similar results were obtained with m3-transfected cells.

whole-cell recording configuration, the electrical properties of the cell rapidly stabilized and remained stable for a couple of hours (Fig. 6*A*). In 13% of cells recorded using the control intracellular solution ($n = 75$) spontaneous activation of outward currents occurred on breaking into the cell. The Petri dishes containing such cells were discarded and only dishes with no recordings of such spontaneously active cells were used for IP_3 and IP_4 experiments.

Inclusion of IP_3 in the intracellular pipette solution induced dose-dependent increases in outward current when the cells were voltage clamped at −50 mV. This increase in current was associated with an increase in conductance (Fig. 6 *B–D*). IP_3 (10 μM) induced small delayed responses in three out of the twelve cells recorded (Fig. 6*B*). The responses lasted about 3s and at −50 mV the average peak current amplitude was 6 ± 1 pA ($n = 2$) in m1-transfected cells. IP_3 (50 μM) induced outward currents (Fig. 6*C*) in 42% of cells examined, producing currents lasting about 10 s with an average peak current amplitude of 43 ± 12 pA ($n = 4$). IP_3 (100 μM) induced

outward currents in 80% of cells tested ($n = 20$) (Fig. 6*D*). These responses lasted about 30 s and had an average peak current of 74 ± 11 pA ($n = 8$), measured at -50 mV in m1-transfected cells. After inclusion of 10 or 50 μM-IP_3 in the intracellular pipette solution, responses to ACh could still be elicited; however, few cells exhibiting

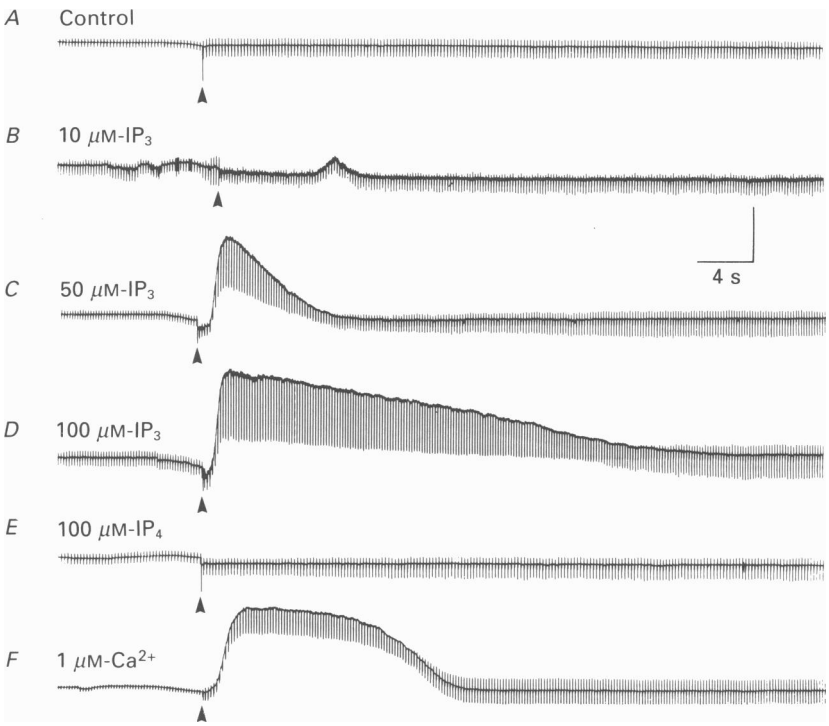

Fig. 6. IP_3 and elevated Ca^{2+} mimic ACh-induced electrical responses. Cells were held originally in the cell-attached mode and recorded from during rupture of the patch (at arrows) into the whole-cell recording configuration (WCR). Traces *A*, *C* and *D* were recorded from cells transfected with m3; *B*, *E* and *F* are traces recorded from A9 L cells transfected with m1. All cells were voltage clamped at -50 mV. *A*, control solutions had no effect on whole-cell current on breaking into WCR mode. *B*, 10 μM-IP_3 produced a delayed, small, transient increase in outward current. *C*, 50 μM- and *D*, 100 μM-IP_3 induced rapidly peaking outward current responses associated with an increase in conductance which lasted only 10–20 s. *E*, 100 μM-IP_4 produced no effect on whole-cell currents. *F*, raising intracellular Ca^{2+} from 20 nM to 1 μM caused an increase in outward current and conductance similar to that activated by IP_3. Vertical calibration 50 pA in *A*, *C*, *D* and *E*; 25 pA in *B*; and 100 pA in *F*.

outward current responses to 100 μM-IP_3 responded to subsequent applications of ACh. Inclusion of 100 μM-IP_4 in the intracellular pipette solution had no effect on membrane properties ($n = 7$) (Fig. 6*E*) and responses to ACh could be elicited in all seven cells. Inclusion of 10–20 μM-IP_4 ($n = 6$) in intracellular solutions already containing 10–100 μM-IP_3 did not appear to effect the IP_3-induced responses (not shown).

Raising the concentration of free Ca^{2+} in the intracellular patch pipette from 20 nM (0·1 mM-Ca^{2+}, 1·1 mM-EGTA) to 1 μM (1 mM-Ca^{2+}, 1·1 mM-EGTA) (Fabiato &

Fabiato, 1979), resulted in rapid activation of an outward current associated with an increase in conductance in 78% of the cells tested ($n = 23$) (Fig. 6*F*), similar to that recorded following intracellular dialysis with IP_3. The conductance measured in m1-transfected cells at the peak of the response to 1 μM-Ca^{2+} dialysis was $4{\cdot}8 \pm 0{\cdot}8$ nS ($n = 9$), calculated from the peak current amplitude at -50 mV, assuming a reversal potential of -65 mV. Current responses to ACh could not subsequently be obtained in 50% of cells tested.

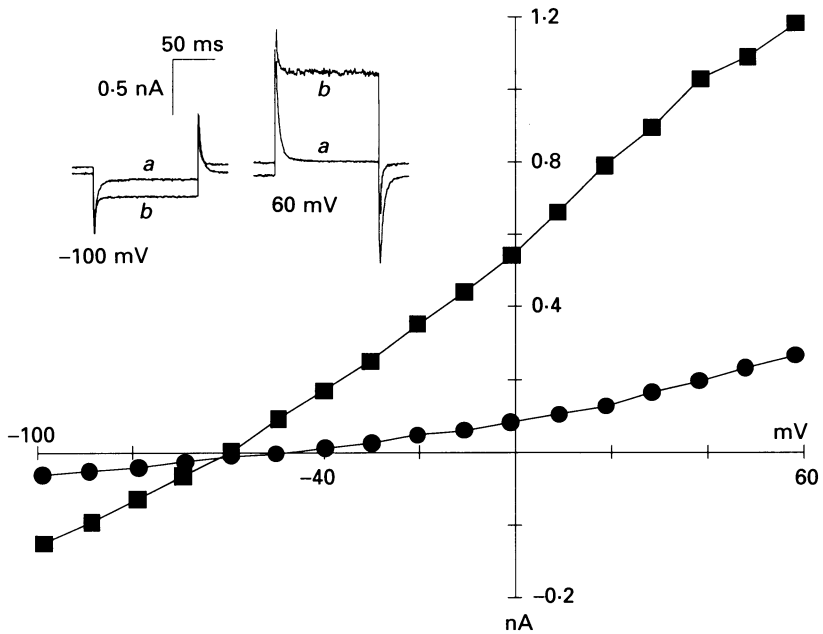

Fig. 7. IP_3 evokes currents similar to those activated by ACh. During the peak of the current responses induced by 100 μM-IP_3, m1-transformed cells were stepped through a range of potentials in 10 mV, 100 ms steps from a holding potential of -50 mV. The current response at the end of the 100 ms step was plotted against potential to construct a current–voltage (*I–V*) curve. Squares (and *b* in the inset) indicate data acquired during IP_3-induced responses; the circles (and *a* in the inset) denote return of the induced current to baseline. The IP_3-induced current reversed at -60 mV, close to the potential at which the ACh-induced current reverses. Peak conductance during the IP_3-induced response was 2·4 nS which declined to a baseline value of 0·3 nS.

The IP_3-induced current reversed at -65 ± 2 mV ($n = 5$) (Fig. 7), which is similar to that obtained with ACh in previous studies (Jones *et al.* 1988*a*, *b*). The peak conductance induced by 100 μM-IP_3 in m1-transfected A9 L cells was somewhat lower than that found previously with ACh (Jones *et al.* 1988*a*, *b*), being increased from $0{\cdot}26 \pm 0{\cdot}09$ nS in recovery to $1{\cdot}66 \pm 0{\cdot}26$ nS ($n = 5$). The conductance was obtained from the slope of the current–voltage curve constructed from current measurements made at a variety of potentials during the plateau phase of the IP_3-induced current. The IP_3-induced current response showed a dependence on K^+ similar to that in the ACh-induced responses (Jones *et al.* 1988*a*, *b*) shifting from -65 ± 2 ($n = 5$) to -19 ± 6 mV ($n = 3$) on increasing the extracellular KCl solution from 5 to 50 mM.

Inclusion of 100 μM-IP_3 in the intracellular pipette solution or increased $[Ca^{2+}]_i$ also induced outward current responses at −50 mV in A9 L cells transformed with m2 ($n = 2$) muscarinic receptors, similar to those activated by m1- or m3-transformed cells.

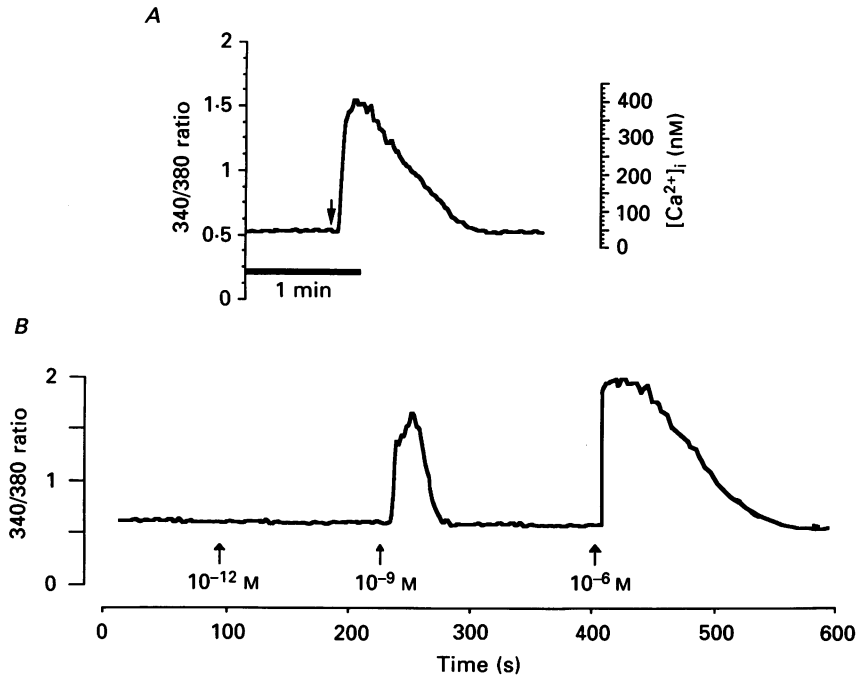

Fig. 8. Fura-2 single-cell measurements show dose-dependent increases in intracellular Ca^{2+} concentration induced by ACh. *A*, bath application of 1 μM-ACh (at arrow) for 10 s increased intracellular Ca^{2+}, after a delay, from resting levels of 50 nM to a peak of about 400 nM. Calcium concentrations were calibrated by measurements in Ca^{2+}-free and 2 mM-Ca^{2+} in the presence of 10 μM ionomycin. *B*, representative responses to three concentrations of ACh applied at the arrows recorded in the same cell show that ACh-induced increases in Ca^{2+} are dose-dependent. The 340/380 ratio in *A* and *B* represents changes in Ca_i^{2+} concentration.

Role and source of Ca^{2+} in the ACh-induced response

A fluorescent Ca^{2+} indicator dye, Fura-2, was used to study single A9 L cells transfected with m1 and m3 muscarinic receptors, to ascertain the role and source of Ca^{2+} in ACh-induced electrical responses. Bath application of 1 μM-ACh for 10 s caused a rapid rise in Ca^{2+}, from a resting level of about 50 nM to around 400 nM (Fig. 8*A*). The response peaked within 20 s and declined over a period of 1–1·5 min back to the resting level. Reproducible increases in Ca^{2+} were induced by ACh when applied every 3 min in this manner. Continued application of ACh to the cells did not greatly prolong the rise in Ca^{2+}, suggesting that some desensitization had occurred. The relationship between ACh concentration and Ca^{2+} response is shown in Fig. 8*B*.

The ACh-induced increases in Ca^{2+} were due to activation of muscarinic receptors as they were reversibly inhibited by 1 μM-atropine ($n = 5$) (Fig. 9*A*).

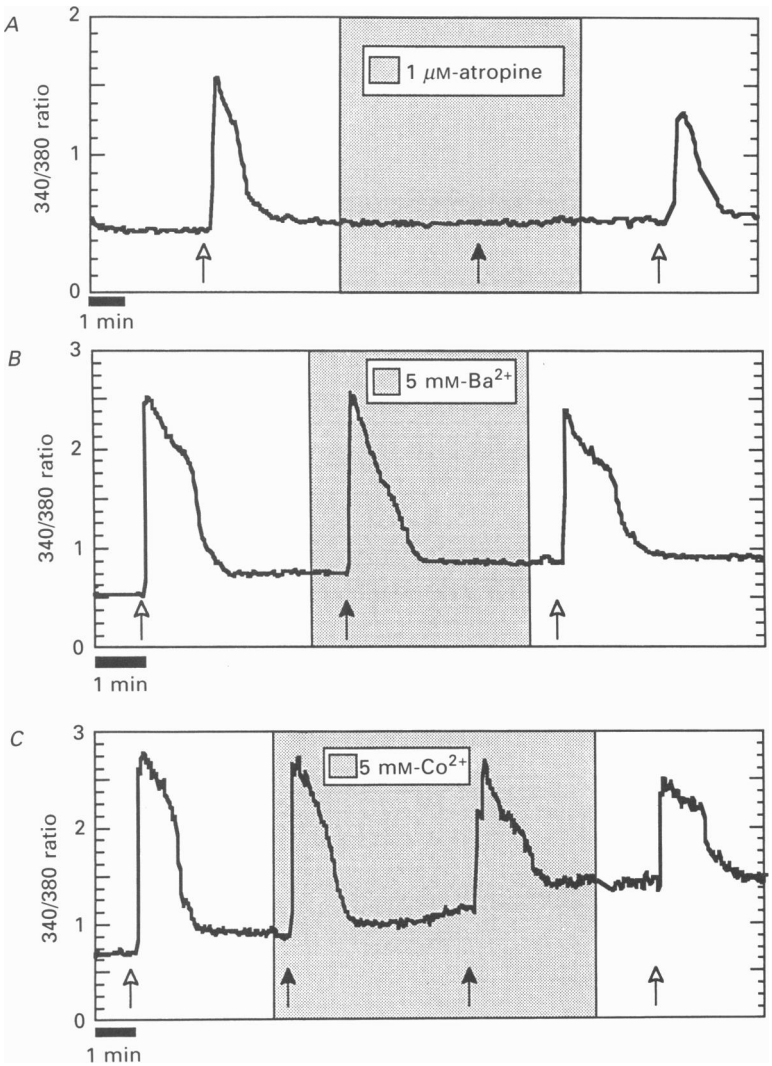

Fig. 9. ACh-induced Ca_i^{2+} responses are muscarinic in nature. *A*, application of 1 μM-atropine to the bathing solution completely abolished the ACh-induced Ca_i^{2+} response. *B*, application of 5 mM-barium had essentially no effect on ACh-induced Ca^{2+} responses though both 340 and 380 nm fluorescence levels were lowered. *C*, 5 mM-cobalt slightly reduced the Ca^{2+} response and irreversibly lowered the fluorescence levels at both 340 and 380 nm; however, the 380 signal was reduced to a greater extent than the 340, accounting for the upward drift of the baseline ratio. The m1- and m3-transformed cells gave qualitatively similar results.

Barium (5 mM) did not appear to affect the ACh-induced increases in Ca^{2+} ($n = 4$) (Fig. 9*B*), though it had a slight quenching effect on the 380 nm excitation free-Fura-2 signal, suggesting that it entered the cell and bound to the Fura-2. Cobalt (5 mM) appeared to reduce the ACh-induced Ca^{2+} response ($n = 5$) (Fig. 9*C*), but it also irreversibly quenched the Fura-2 signal. The Fura-2 fluorescence was reduced by Co^{2+} and Ba^{2+} at both excitation wavelengths but the 380 nm excitation was reduced

to a greater extent than that at 340 nm. This accounts for the rising baseline ratio level. However, the results indicate that the Ba^{2+} had little effect and that Co^{2+} produced a small reduction in the ACh-induced Ca^{2+} response.

The role of extracellular Ca^{2+} in the ACh-induced Ca^{2+} response was investigated.

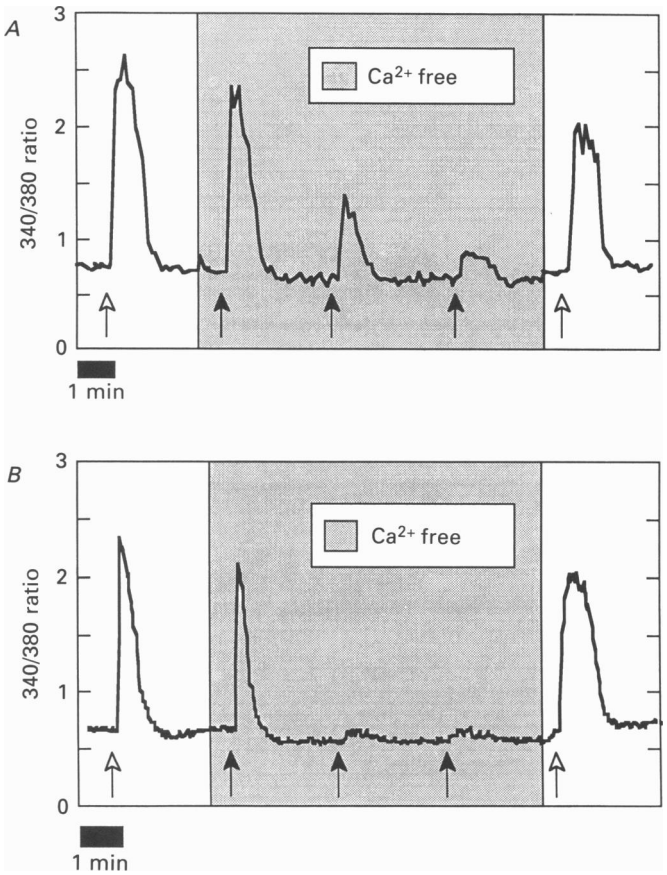

Fig. 10. ACh-induced Ca_i^{2+} responses have extracellular Ca^{2+} requirements. Initial ACh-induced responses were only slightly reduced on exposure to Ca^{2+}-free medium. *A*, repeated ACh responses slowly declined. *B*, repeated applications of ACh produced dramatically reduced responses. Return to control medium containing 2 mM-Ca^{2+} rapidly returned the Ach-induced Ca_i^{2+} responses to control levels. No qualitative differences were noted between m1- and m3-transfected cells.

The first response to ACh was only slightly reduced or was unaffected by the removal of extracellular Ca^{2+} ($n = 16$) (Fig. 10). Subsequent applications of ACh produced a reduction in the Ca^{2+} response over 5–15 min ($n = 16$) (Fig. 10*A* and *B*). On restoring Ca^{2+} to the extracellular solution, the ACh-induced Ca^{2+} response rapidly recovered to control levels. Prolongation of the period between removal of extracellular Ca^{2+} and the initial application of ACh from about 1·5 min to around 5 min led to a reduction in the initial ACh-induced response. It is unlikely that this period is required to exchange the bath solution to one of Ca^{2+}-free medium, as a flow rate of 3 ml min^{-1} exchanges the 100 μl bath volume thirty times per minute; thus it is

suggested that this is the time required to deplete intracellular Ca^{2+} stores. Therefore, it would appear that although an initial increase in Ca^{2+} can be elicited by ACh in Ca^{2+}-free solutions, extracellular Ca^{2+} is necessary for continued robust responses.

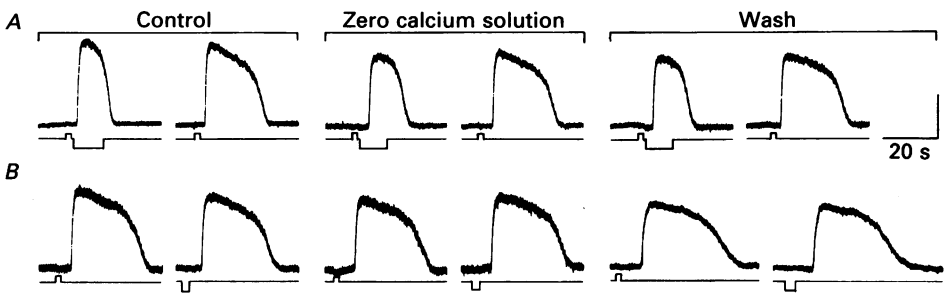

Fig. 11. ACh-induced electrical responses are not dependent on extracellular Ca^{2+}. ACh-induced responses were obtained in A9 L cells transfected with the m1 muscarinic receptor voltage clamped at −30 mV. *A*, the first response to ACh (10 μM in Ca^{2+}-free medium, upward deflection) was followed by pressure ejection application of control medium containing 2 mM-Ca^{2+} from a second pipette placed close to the cell (downward deflection). Removal of extracellular Ca^{2+}, by addition of 1·1 mM-EGTA followed by perfusion of the bath with Ca^{2+}-free medium, slightly reduced the ACh-induced responses; however, the amplitudes were the same in Ca^{2+}-free medium whether Ca^{2+} was applied or not. *B*, ACh was applied from two pipettes, one containing 2 mM-Ca^{2+} (upward deflection) and the other containing Ca^{2+}-free medium (downward deflection). Removal of extracellular Ca^{2+} had no effect on either ACh-induced current. Vertical calibration: *A*, 50 pA; *B*, 25 pA.

The role of extracellular Ca^{2+} in the generation of ACh-elicited electrical responses was investigated. Removal of extracellular Ca^{2+} appeared to produce only very slight reductions in ACh-induced responses. Consistent current responses were obtained on application of 10 μM-ACh dissolved in Ca^{2+}-free medium from a pressure ejection pipette (Fig. 11*A*). Applications of normal medium containing 2 mM-Ca^{2+} from a second pressure ejection pipette followed alternate ACh applications. In control (2 mM-Ca^{2+}) solutions the responses to ACh were of equal amplitude and were only slightly reduced by removal of Ca^{2+} from the bathing medium (Fig. 11*A*); however, both ACh-induced responses either with or without a supply of Ca^{2+} were identical in amplitude. Removal of Ca^{2+} from the medium was performed firstly by addition of 1·1 mM-EGTA to the bathing medium, followed by perfusion of the bath with Ca^{2+}-free medium. Extracellular Ca^{2+} does not appear to contribute to the electrical response, but Ca^{2+} may be required at the time of application of ACh, so a second protocol was employed.

Equal amplitude responses to 10 μM-ACh were obtained from two pressure pipettes, one containing 10 μM-ACh in Ca^{2+}-free medium, the other containing 10 μM-ACh in control medium with 2 mM-Ca^{2+} (Fig. 11*B*). The responses to ACh applied in 2 mM-Ca^{2+} or Ca^{2+}-free solution were the same and neither were reduced compared to each other when the solution was changed to one containing no Ca^{2+} and 1·1 mM-EGTA. Thus removal of extracellular Ca^{2+} had no effect on the ACh-induced current responses.

DISCUSSION

It is concluded that m1 and m3 muscarinic receptors activate Ca^{2+}-dependent conductances via a pertussis toxin-insensitive G protein. The response to activation of m1 and m3 receptors in NG108-15 cells was also not pertussis toxin sensitive (Fukuda *et al.* 1988). Activation of a pertussis toxin-insensitive G protein results in an increase in IP_3 in m1- and m3-transformed A9 L cells (Brann *et al.* 1988) and intracellular application of IP_3 was shown to mimic the ACh-induced current response. Many systems have shown the involvement of IP_3 in activation of Ca^{2+}-dependent K^+ or Cl^- conductances, for example, in NG108-15 cells (Higashida & Brown, 1986; Brown & Higashida, 1988), in lacrimal glands (Evans & Marty, 1986; Morris, Gallacher, Irvine & Petersen, 1987) and in *Xenopus* oocytes (Oron, Dascal, Nadler & Lupu, 1985; Nomura, Kaneko, Kato, Yamagishi & Sugiyama, 1987). Increasing the concentration of intracellular free Ca^{2+} also mimicked the ACh-induced current response. Taken together the results suggests that IP_3 mediates the effect of ACh in m1- and m3-transformed A9 L cells by mobilizing Ca^{2+} from internal stores. Although there was no requirement for extracellular Ca^{2+} in the generation of the electrical response, most of the ACh-induced Ca_i^{2+} response disappeared within minutes of removing extracellular Ca^{2+}. The m1 and m3 muscarinic electrical and optical responses were qualitatively similar.

ACh-activated channels

Acetylcholine activates two types of K^+ channel activity (36 and 5 pS), which though apamin sensitive and not voltage dependent (Jones *et al.* 1988*a*), do not correlate with the 'SK' type channels reported by Blatz & Magleby (1986, 1987), nor with the Ca^{2+}-activated channels recorded from hepatocytes (Capiod & Ogden, 1989). The 36 pS channel appears to be closely related to the channel activated by bradykinin and IP_3 in NG108-15 cells (Higashida & Brown, 1988). The Ca^{2+}-dependent channels recorded from m1- and m3-transformed NG108-15 cells by Neher, Marty, Fukuda, Kubo & Numa (1988) appear to be similar to the 5 pS channel activity of this study, but these were recorded in different K^+ concentrations. Both the 5 and 36 pS channels differ from those activated by ACh in exocrine glands, which are the large, maxi or BK channels (for reviews see Petersen, 1986; Blatz & Magleby, 1987). The third species of channel activated by ACh, active in the cell-attached patch mode at 0 mV, probably involves Cl^- ions and is currently being investigated.

Role of Ca^{2+}

The Fura-2 data showed that application of ACh increased intracellular Ca^{2+} in A9 L cells transfected with m1 and m3 muscarinic receptors. Stimulation of m1 and m3-transfected NG108-15 cells likewise raised intracellular Ca^{2+} concentrations (Neher *et al.* 1988).

The removal of Ca^{2+} from the extracellular medium appeared to deplete internal stores. This depletion had no effect on the ACh-induced electrical response. Thus, it would appear that the small residual rise in intracellular Ca^{2+} induced by ACh in

Ca^{2+}-free extracellular medium was sufficient to activate the Ca^{2+}-dependent conductances. Intracellular Ca^{2+} is buffered to around 20 nM with EGTA in the patch-clamp recordings and calibration of the Fura-2 signal shows resting Ca^{2+} to be about 50 nM; thus the calcium levels are comparable. In the electrical studies, however, there is a continual supply of Ca^{2+} from the patch pipette and therefore run-down of intracellular stores in the absence of extracellular Ca^{2+} is unlikely. Thus, a direct comparison between the two methods is not possible. Simultaneous measurements of the Ca^{2+} concentration and electrical response would clarify this result.

The concentration dependence of the ACh-induced electrical response appeared to be all-or-none, with channels maximally activated at concentrations above 20 nM. This observation is probably related to the calcium concentration reaching a threshold value at which the calcium-dependent channels activate (Evans & Marty, 1986; Marty, Evans, Tan & Trautmann, 1986). Horn & Marty (1988) showed that 50 nM-ACh elicited submaximal responses and that current amplitude responses peaked at about 1 μM-ACh in lacrimal glands. The differences in the results suggests that the channels of this study activate at lower Ca^{2+} concentrations, but it must be borne in mind that higher concentrations of calcium buffer were used in the intracellular solution of the present study and that there are differences in the extent of dialysis of the cell due to the different methods of obtaining a whole cell recording.

The ACh-induced Ca^{2+} response on the other hand could be activated by ACh concentrations well below 20 nM, but a direct comparison of the electrical recordings to those of the calcium measurements is made difficult by the EGTA buffering of the intracellular Ca^{2+} in the electrical experiments. Reductions in ACh-induced Ca^{2+} responses, similar to those of the present study, have also been observed on removal of extracellular Ca^{2+} in cultured hippocampal neurons (Kudo, Ogura & Iijima, 1988). The m1- and m3-stimulated rise in intracellular Ca^{2+}, however, was not dependent on extracellular Ca^{2+} in NG108-15 cells (Neher *et al.* 1988) suggesting differences in Ca^{2+} storage and mobilization among different cell types.

As it would appear that Ca^{2+} entry is required to maintain Ca^{2+} stores in A9 L cells, this might help to explain the entry of barium and cobalt into the cell. Barium had a small quenching action on the Fura-2 ratio but did not affect the Ca_i^{2+} response. Thus barium entered the cell and blocked the Ca^{2+}-dependent K^+ channel as would be predicted. Cobalt on the other hand may block Ca^{2+} channels in the cell membrane, which may explain the small reduction in Ca^{2+} response, but must also have entered the cell in order to quench the Fura-2 signal. The inhibition of the ACh-induced Ca^{2+}-dependent conductances by cobalt (Jones *et al.* 1988*a*, *b*) may be due to it blocking the Ca^{2+} binding site at the Ca^{2+}-dependent K^+ channel.

Desensitization

The ACh-induced electrical responses desensitized within about 25 s during constant application of ACh to the cells. The current responses induced by intracellular 100 μM-IP_3 also declined with a similar time course, suggesting that the desensitization occurred at a step beyond IP_3 production. This suggestion was supported by the time course of the decline in the ACh-induced Ca^{2+} response, which took several minutes to return to baseline during constant application of agonist.

Thus the desensitization of the electrical response must take place after the release of Ca^{2+}. This was borne out by the time course of desensitization of the electrical response induced by raised intracellular Ca^{2+}. In fact, using concentrations of intracellular Ca^{2+} as high as 1 μM caused a desensitization of the outward current response somewhat faster than that observed with IP_3. From the Fura-2 calibrations, application of 1 μM-ACh resulted in maximal increases in Ca^{2+} from 50 nM to around 400 nM; thus, 1 μM-Ca^{2+} is probably saturating. Application of ACh to cells dialysed with 100 μM-IP_3 or 1 μM-free Ca^{2+} often did not evoke conductance increases, possibly due to the continued inactivation of the K^+ channels by elevated Ca^{2+}.

The authors would like to thank J. Dempster for his helpful suggestions on the analysis of the single-channel data.

REFERENCES

BLATZ, A. L. & MAGLEBY, K. L. (1986). Single apamin-blocked calcium-activated potassium channels of small conductance in cultured rat skeletal muscle. *Nature* **323**, 718–720.

BLATZ, A. L. & MAGLEBY, K. L. (1987). Calcium-activated potassium channels. *Trends in Neurological Sciences* **11**, 463–467.

BONNER, T. I., BUCKLEY, N. J., YOUNG, A. C. & BRANN, M. R. (1987). Identification of a family of muscarinic ACh receptor genes. *Science* **237**, 527–532.

BONNER, T. I., YOUNG, A. C., BRANN, M. R. & BUCKLEY, N. J. (1988). Cloning and expression of the human and rat m5 muscarinic ACh receptor genes. *Neuron* **1**, 403–410.

BRANN, M. R., BUCKLEY, N. J., JONES, S. V. P. & BONNER, T. I. (1987). Expression of a cloned muscarinic receptor in A9 L cells. *Molecular Pharmacology* **32**, 350–355.

BRANN, M. R., CONKLIN, B., DEAN, N. M., COLLINS, R. M., BONNER, T. I. & BUCKLEY, N. J. (1988). Cloned muscarinic receptors couple to different G-proteins and second messengers. *Society for Neuroscience Abstracts* **14**, 600.

BROWN, D. A. (1986). ACh and brain cells. *Nature* **319**, 358–359.

BROWN, D. A. & HIGASHIDA, H. (1988). Inositol 1,4,5-trisphosphate and diacylglycerol mimic bradykinin effects on mouse neuroblastoma × rat glioma hybrid cells. *Journal of Physiology* **397**, 185–207.

CAPIOD, T. & OGDEN, D. C. (1989). The properties of calcium-activated potassium ion channels in guinea-pig isolated hepatocytes. *Journal of Physiology* **409**, 285–295.

CHRISTIE, M. J. & NORTH, R. A. (1988). Control of ion conductances by muscarinic receptors. *Trends in Pharmacological Sciences*, suppl. 3, 30–34.

CONKLIN, B. R., BRANN, M. R., BUCKLEY, N. J., MA, A. L., BONNER, T. I. & AXELROD, J. (1988). Stimulation of arachidonic acid release and inhibition of mitogenesis by cloned muscarinic receptor subtypes stably expressed in A9 L cells. *Proceedings of the National Academy of Sciences of the USA* **85**, 8698–8702.

DEMPSTER, J. (1988). Computer analysis of electrophysiological signals. In *Microcomputers in Physiology*, ed. FRASER, P. J. pp. 51–93. IRL Press, Oxford, Washington D.C.

DI VIRGILIO, F., STEINBERG, T. H., SWANSON, J. A. & SILVERSTEIN, S. C. (1988). Fura-2 secretion and sequestration in macrophages. A blocker of organic anion transport reveals that these processes occur via a membrane transport system for organic anions. *Journal of Immunology* **140**, 915–920.

EVANS, M. G. & MARTY, A. (1986). Potentiation of muscarinic and α-adrenergic responses by an analogue of guanosine 5′-triphosphate. *Proceedings of the National Academy of Sciences of the USA* **83**, 4099–4103.

FABIATO, A. & FABIATO, F. (1979). Calculator programs for computing the composition of the solutions containing multiple metals and ligands used for experiments in skinned muscle cells. *Journal de physiologie* **75**, 463–505.

FORSYTHE, I. D. & COATES, R. T. (1988). A chamber for electrophysiological recording from cultured neurones allowing perfusion and temperature control. *Journal of Neuroscience Methods* **25**, 19–27.

FUKUDA, K., HIGASHIDA, H., KUBO, T., MAEDA, A., AKIBA, I., BUJO, H., MISHINA, M. & NUMA, S. (1988). Selective coupling with K^+ currents of muscarinic ACh receptor subtypes in NG108-15 cells. *Nature* **335**, 355–358.

FUKUDA, K., KUBO, T., AKIBA, I., MAEDA, A., MISHINA, M. & NUMA, S. (1987). Molecular distinction between muscarinic subtypes. *Nature* **327**, 623–625.

GRYNKIEWCZ, G., POENIE, M. & TSIEN, R. Y. (1985). A new generation of calcium indicators with greatly improved fluorescence properties. *Journal of Biological Chemistry* **260**, 3440–3450.

HAMILL, O. P., MARTY, A., NEHER, E., SAKMANN, B. & SIGWORTH, F. (1981). Improved patch-clamp techniques for high-resolution current recording from cells and cell-free membrane patches. *Pflügers Archiv* **391**, 85–100.

HARDEN, T. K., TANNER, L. I., MARTIN, M. W., NAKAHATA, N., HUGHES, A. R., HEPLER, J. R., EVANS, T., MASTERS, S. B. & BROWN, J. H. (1986). Characteristics of two biochemical responses to stimulation of muscarinic cholinergic receptors. *Trends in Pharmacological Sciences*, suppl. 7, 14–18.

HIGASHIDA, H. & BROWN, D. A. (1986). Two polyphosphatidyl-inositide metabolites control two K^+ currents in a neuronal cell. *Nature* **323**, 333–335.

HIGASHIDA, H. & BROWN, D. A. (1988). Ca^{2+}-dependent K^+ channels in neuroblastoma hybrid cells activated by intracellular inositol trisphosphate and extracellular bradykinin. *FEBS Letters* **238**, 395–400.

HORN, R. & MARTY, A. (1988). Muscarinic activation of ionic currents measured by a new whole-cell recording method. *Journal of General Physiology* **92**, 145–159.

JONES, S. V. P., BARKER, J. L., BONNER, T. I., BUCKLEY, N. J. & BRANN, M. R. (1988*a*). Electrophysiological characterization of cloned m1 muscarinic receptors expressed in A9 L cells. *Proceedings of the National Academy of Sciences of the USA* **85**, 4056–4060.

JONES, S. V. P., BARKER, J. L., BUCKLEY, N. J., BONNER, T. I., COLLINS, R. M. & BRANN, M. R. (1988*b*). Cloned muscarinic receptor subtypes expressed in A9 L cells differ in their coupling to electrical responses. *Molecular Pharmacology* **34**, 421–426.

JONES, S. V. P., GOODMAN, M. B., BARKER, J. L. & BRANN, M. R. (1989*a*). IP_3 mediates m1 and m3 muscarinic receptor-activated calcium-dependent conductances. *Biophysical Journal* **55**, 66a.

JONES, S. V. P., MURPHY, T. J. & BRANN, M. R. (1989*b*). Physiological comparison of cloned muscarinic receptor subtypes expressed in CHO cells. *Trends in Pharmacological Sciences* (in the Press).

KUBO, T., FUKUDA, K., MIKAMI, A., MAEDA, A., TAKAHASHI, H., MISHINA, M., HAGA, K., HAGA, T., ICHIYAMA, A., KANGAWA, K., KOJIMA, M., MATSUO, H., HIROSE, T. & NUMA, S. (1986). Cloning, sequencing and expression of complementary DNA encoding the muscarinic ACh receptor. *Nature* **323**, 411–416.

KUBO, T., MAEDA, A., SUGIMOTO, K., AKIBA, I., MIKAMI, A., TAKAHASHI, H., HAGA, T., HAGA, K., ICHIYAMA, A., KANGAWA, K., MATSUO, H., HIROSE, T. & NUMA, S. (1987). Primary structure of porcine cardiac muscarinic ACh receptor deduced from the cDNA sequence. *FEBS Letters* **209**, 367–372.

KUDO, Y., OGURA, A. & IIJIMA, T. (1988). Stimulation of muscarinic receptors in hippocampal neuron induces characteristic increase in cytosolic free Ca^{2+} concentration. *Neuroscience Letters* **85**, 345–350.

MARTY, A., EVANS, M. G., TAN, Y. P. & TRAUTMANN, A. (1986). Muscarinic response in rat lacrimal glands. *Journal of Experimental Biology* **124**, 15–32.

MORRIS, A. P., GALLACHER, D. V., IRVINE, R. F. & PETERSEN, O. H. (1987). Synergism of inositol trisphosphate and tetrakisphosphate in activating calcium-dependent potassium channels. *Nature* **330**, 653–655.

NATHANSON, N. M. (1987). Molecular properties of the muscarinic ACh receptor. *Annual Review of Neuroscience* **10**, 195–236.

NEHER, E., MARTY, A., FUKUDA, K., KUBO, T. & NUMA, S. (1988). Intracellular calcium release mediated by two muscarinic receptor subtypes. *FEBS Letters* **240**, 88–94.

NICOLL, R. A. (1988). The coupling of neurotransmitter receptors to ion channels in the brain. *Science* **241**, 545–551.

NOMURA, Y., KANEKO, S., KATO, K., YAMAGISHI, S. & SUGIYAMA, Y. (1987). Inositol phosphate formation and chloride current responses induced by ACh and serotonin through GTP-binding proteins in *Xenopus* oocyte after injection of rat brain messenger RNA. *Molecular Brain Research* **2**, 113–123.

NOVOTNY, E. A. & BRANN, M. R. (1989). Agonist pharmacology of cloned muscarinic receptors. *Trends in Pharmacological Sciences* (in the Press).

ORON, Y., DASCAL, N., NADLER, E. & LUPU, M. (1985). Inositol-1,4,5-trisphosphate mimics muscarinic response in *Xenopus* oocytes. *Nature* **313**, 141–143.

PERALTA, E. G., ASHKENAZI, A., WINSLOW, J. W., SMITH, D. W., RAMACHANDRAN, J. & CAPON, D. J. (1987). Distinct primary structures, ligand-binding properties and tissue-specific expression of four human muscarinic ACh receptors. *EMBO Journal* **6**, 3923–3929.

PERALTA, E. G., ASHKENAZI, A., WINSLOW, J. W., RAMACHANDRAN, J. & CAPON, D. J. (1988). Differential regulation of PI hydrolysis and adenylyl cyclase by muscarinic receptor subtypes. *Nature* **334**, 434–437.

PETERSEN, O. H. (1986). Calcium-activated potassium channels and fluid secretion by exocrine glands. *American Journal of Physiology* **251**, G1–13.